

Nuclear structure theory

Thomas Papenbrock



and

OAK RIDGE NATIONAL LABORATORY

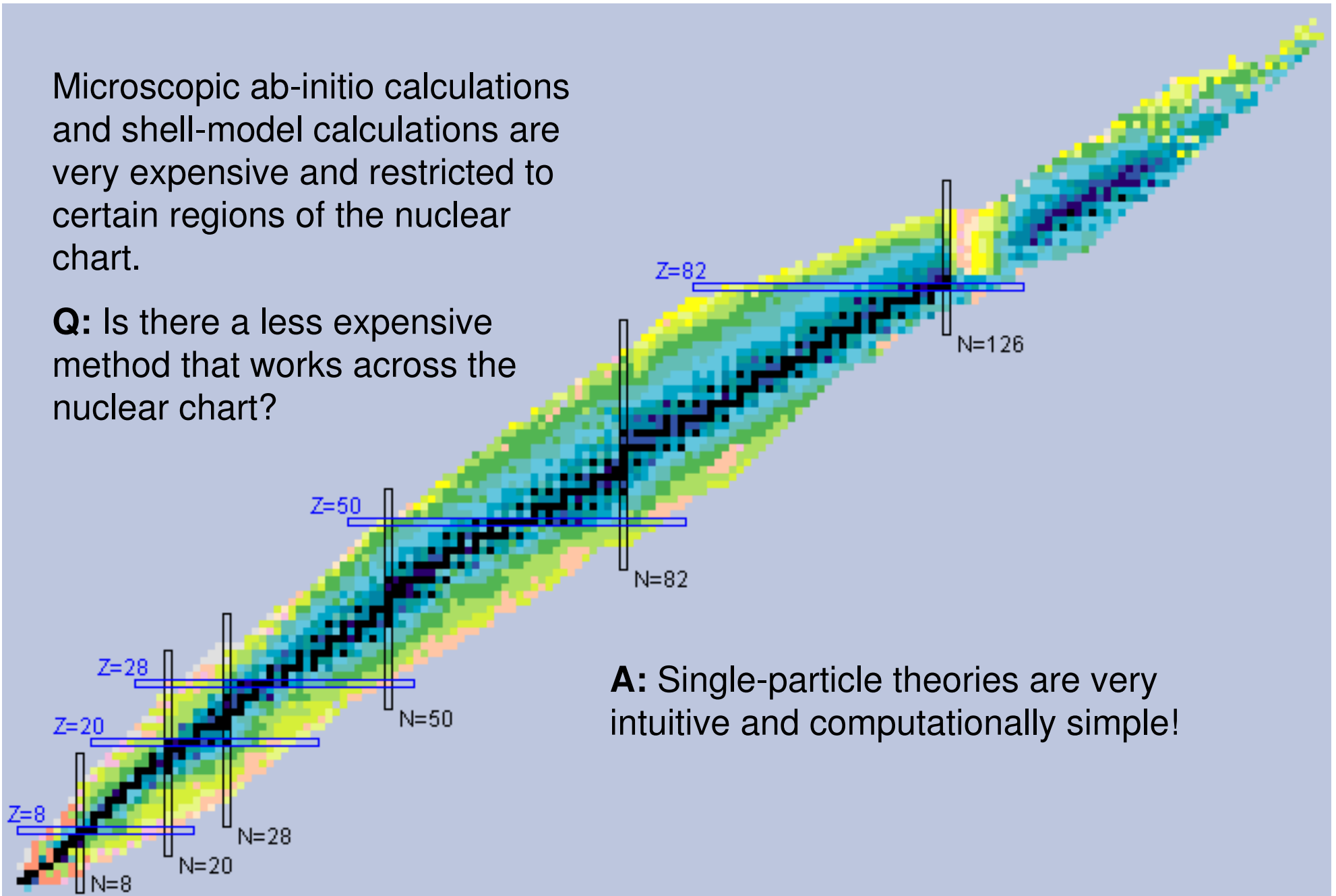
Lecture 3: Self-consistent mean-field and single-particle methods

RIA 2006 Summer School at Oak Ridge

Theoretical method for the entire nuclear chart ?

Microscopic ab-initio calculations and shell-model calculations are very expensive and restricted to certain regions of the nuclear chart.

Q: Is there a less expensive method that works across the nuclear chart?



A: Single-particle theories are very intuitive and computationally simple!



Nobel Prize in chemistry 1998



Walter Kohn

"for his development of
the density-functional
theory"

Two quotes from Kohn's Nobel lecture:

I begin with a provocative statement. *In general the many-electron wavefunction $\Psi(r_1, \dots, r_N)$ for a system of N electrons is not a legitimate scientific concept, when $N \geq N_0$, where $N_0 \approx 10^3$.*

I will use two criteria for defining "legitimacy": a) That Ψ can be calculated with sufficient accuracy and b) can be recorded with sufficient accuracy.

In concluding this section I remark that DFT, while *derived* from the N-particle Schroedinger equation, is finally expressed entirely in terms of the density $n(r)$, in the Hohenberg-Kohn formulation,^[1] and in terms of $n(r)$ and *single-particle* wavefunctions $\psi_j(r)$, in the Kohn-Sham formulation^[2]. This is why it has been most useful for systems of very many electrons where wavefunction methods encounter and are stopped by the "exponential wall".

Density-functional theory (DFT)

- **Hohenberg-Kohn Theorems:** [P. Hohenberg & W. Kohn, Phys. Rev. 136 (1964) B864]
 1. *The ground state electron density of a many electron system in the presence of an external potential uniquely determines the external potential.*
 2. *The functional for the ground state energy is minimized by the ground state electron density.*
- **Comments:**
 - Remark: A functional maps functions to real numbers.
 - Existence theorem only. No simple constructive recipe. What is the energy density functional for nuclei?
- **Example:** Energy of a non-interacting Fermi gas in external potential

$$E[\rho] = \int d^3r \left(\underbrace{\frac{3}{10} (3\pi^2)^{2/3} \frac{\hbar^2}{2m} \rho^{5/3}(r)}_{\text{kinetic energy density (Thomas-Fermi approximation)}} + V_{\text{ext}}(r) \rho(r) \right)$$

energy functional

kinetic energy density
(Thomas-Fermi approximation)

external potential

- **Remark:** HK not a practical tool. Local approximations of the density functional are too inaccurate.

Kohn-Sham DFT [W. Kohn & L. Sham, Phys. Rev. 140 (1965) A1133]

- Kohn-Sham: The form of the density functional is

$$E[\rho] = \int d^3r (\tau(r) + V_{\text{ext}}(r)\rho(r)) + E_{\text{int}}[\rho]$$

$$\rho(r) = \sum_{k=1}^A |\psi_k(r)|^2 \quad \text{density}$$

$$\tau(r) = \frac{\hbar^2}{2m} \sum_{k=1}^A |\nabla\psi_k(r)|^2 \quad \text{kin. energy density (nonlocal!)}$$

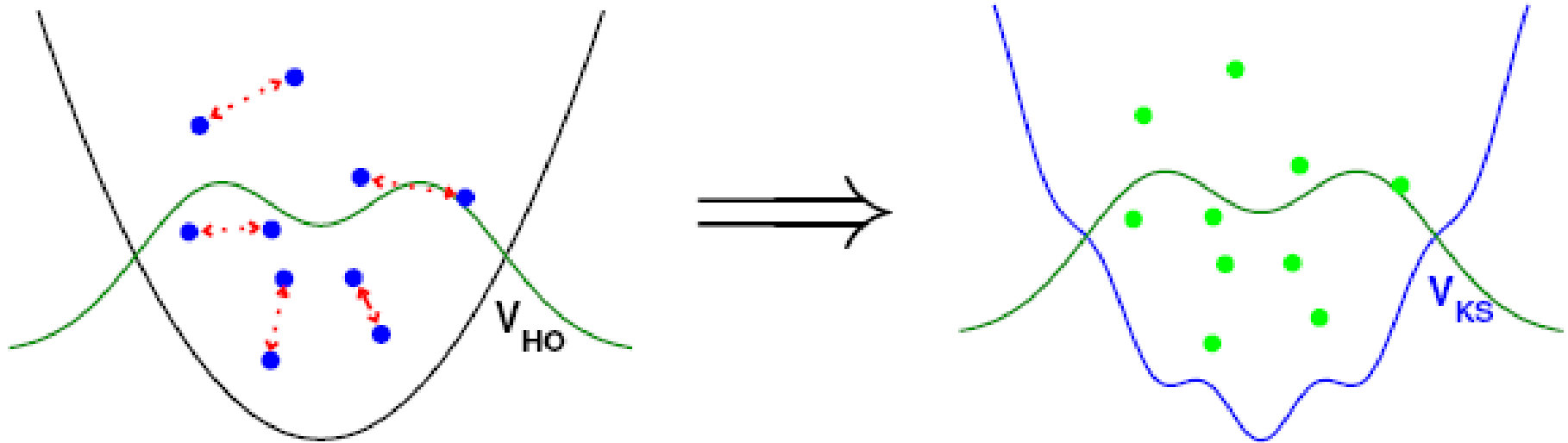
- Kohn-Sham equations: $\delta E[\rho] = 0$

$$\left(-\frac{\hbar^2}{2m} \Delta + \frac{\delta E_{\text{int}}[\rho]}{\delta \rho(r)} + V_{\text{ext}}(r) \right) \psi_k(r) = \mu \psi_k(r)$$

- Remarks: Single-particle Schroedinger equation has to be solved.
- For nuclei, one uses the *local density approximation* (LDA), and gradient corrections.

$$E_{\text{int}} = E_{\text{int}}[\rho, \nabla\rho] = \int d^3r \mathcal{E}(\rho, \nabla\rho)$$

Idea behind DFT



Ground state density of interacting fermions in external harmonic trap.

Turn off the interaction, but change external potential such that the density remains that of the interacting system. The additional potential is the KS potential.

Systematic construction of density functional for dilute Fermi gas

Dilute Fermi gas:

All parameters of the potential (scattering length, effective range, ...) much smaller than the Fermi wave length (or average two-particle distance) \rightarrow small expansion parameter exist, namely $\mathbf{k}_F \mathbf{a}$.

Use EFT to systematically construct energy density functional in terms of these small parameters.

$$\mathcal{E} = \rho \frac{\hbar^2 k_F^2}{2m} \left\{ \frac{3}{5} + \underbrace{\left[\frac{2}{3\pi} k_F a + \frac{4}{35\pi^2} (11 - 2 \log 2) (k_F a)^2 \right]}_{\text{Contributions from interaction}} \right\}$$
$$\rho = \frac{k_F^3}{3\pi^2}$$

Contributions from interaction

This systematic approach gives valuable insights into the construction of density functionals. However, it is at present limited to “solvable” Hamiltonians.

See, e.g., R. J. Furnstahl and H.-W. Hammer, *Annals Phys.* 302 (2002) 206.

S. J. Puglia et al, *Nucl.Phys.* A723 (2003) 145.

Skyrme Hartree Fock theory

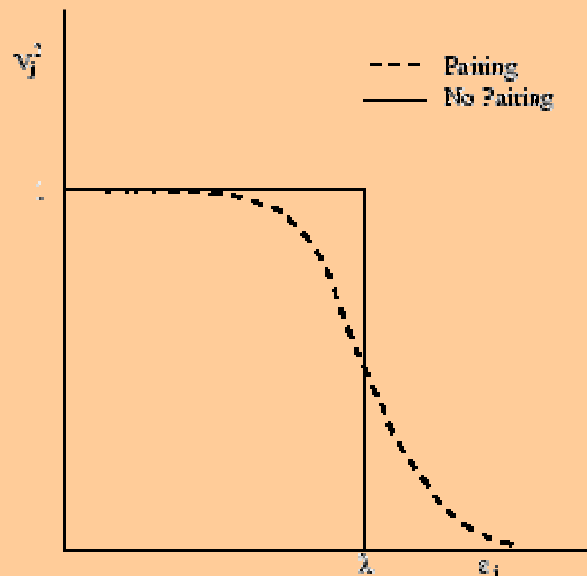
Refs.: T.H.R. Skyrme, Phil. Mag. 1 (1956) 1043; D. Vautherin and D. M. Brink, PRC 5 (1972) 626; J. W. Negele and D. Vautherin, PRC 5 (1972) 1472.

Main idea: Use mean-field Hamiltonian that depends on densities and currents, and solve self-consistently.

$$\begin{aligned}
 E &= \int d^3r n \{ \mathcal{E}_{\text{kin}} + \mathcal{E}_{\text{Skyrme}} + \mathcal{E}_{\text{Skyrme,odd}} \} + E_{\text{Coulomb}} + E_{\text{pair}} + E_{\text{cm}} \quad , \\
 n\mathcal{E}_{\text{kin}} &= \frac{\hbar^2}{2m} \int d^3\tau \quad , \\
 n\mathcal{E}_{\text{Skyrme}} &= \frac{B_0 + B_3 n^\alpha}{2} n^2 - \frac{B'_0 + B'_3 n^\alpha}{2} \tilde{n}^2 \\
 &\quad + B_1 (n\tau - \mathbf{j}^2) - B'_1 (\tilde{n}\tilde{\tau} - \tilde{\mathbf{j}}^2) - \frac{B_2}{2} n \Delta n + \frac{B'_2}{2} \tilde{n} \Delta \tilde{n} \\
 &\quad - B_4 n \nabla \cdot \mathbf{J} - (B_4 + B'_4) \tilde{n} \nabla \cdot \tilde{\mathbf{J}} + \frac{C_1}{2} \mathbf{J}^2 - \frac{C'_1}{2} \tilde{\mathbf{J}}^2 \quad , \\
 n\mathcal{E}_{\text{Skyrme,odd}} &= -\frac{C_0 + C_3 n^\alpha}{2} \boldsymbol{\sigma}^2 + \frac{C'_0 + C'_3 n^\alpha}{2} \tilde{\boldsymbol{\sigma}}^2 + \frac{C_2}{2} \boldsymbol{\sigma} \cdot \Delta \boldsymbol{\sigma} - \frac{C'_2}{2} \tilde{\boldsymbol{\sigma}} \cdot \Delta \tilde{\boldsymbol{\sigma}} \\
 &\quad - C_1 \boldsymbol{\sigma} \cdot \boldsymbol{\tau} + C'_1 \tilde{\boldsymbol{\sigma}} \cdot \tilde{\boldsymbol{\tau}} - B_4 \boldsymbol{\sigma} \cdot (\nabla \times \mathbf{j}) - (B_4 + B'_4) \tilde{\boldsymbol{\sigma}} \cdot (\nabla \times \tilde{\mathbf{j}}) \quad , \\
 E_{\text{Coulomb}} &= e^2 \frac{1}{2} \int d^3r d^3r' \frac{n_{\text{p}}(\mathbf{r}) n_{\text{p}}(\mathbf{r}')}{|\mathbf{r} - \mathbf{r}'|} - \frac{3}{4} e^2 \left(\frac{3}{\pi} \right)^{1/3} \int d^3r [n_{\text{p}}]^{4/3} \quad .
 \end{aligned}$$

Pairing in mean-field description: Hartree-Fock-Bogoliubov (HFB) theory

- Attractive interactions destabilize the Fermi-surface with respect to pair correlations, i.e. paired system has lower energy.



- Within HFB theory, vacuum state is product of quasi-particle states.

$$\hat{c}_j = \sum_i (U_{ji}\hat{a}_i + V_{ji}\hat{a}_i^\dagger)$$

$$\{\hat{c}_i, \hat{c}_j^\dagger\} = \delta_{ij} = \{\hat{a}_i, \hat{a}_j^\dagger\}$$

Theory explains BCS-superconductivity. Pairing gaps in even-even nuclei, reduced moments of inertia, etc.

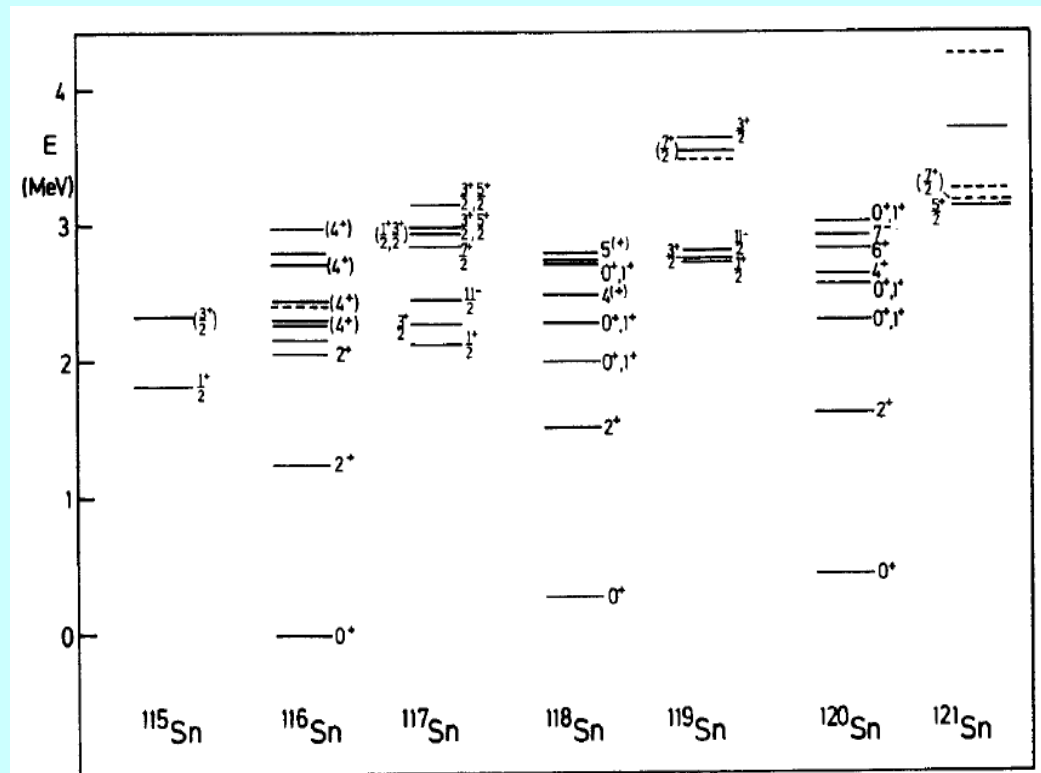


Figure 6.1. Excitation spectra of the $_{50}\text{Sn}$ isotopes.

From: Ring & Schuck, The nuclear many-body problem.

Reminder: Symmetry-breaking in mean-field theories

- HF states usually break symmetries, e.g., translational invariance and rotational invariance.
- HFB quasi-particle states do not exhibit a definite number of particles.
- The breaking of symmetry is desired, as it allows the single-particle state to capture relevant correlations.
- Restoration of symmetries becomes an important issue.

Publicly available program

HFODD

J. Dobaczewski et al, Computer Physics Communications 167 (2005) 214

<http://www.fuw.edu.pl/%7Edobaczew/hfodd/hfodd.html>

Relativistic mean-field (RMF) theory

Relativistic models

- explain large spin-orbit splitting (large scalar and vector potentials).
- explain pseudo-spin symmetry.
- somewhat more constrained than non-relativistic models.

Relativistic Lagrangian: free **nucleons**, free **mesons**, and **interactions**.

$$\begin{aligned}\mathcal{L} = & \bar{\psi} (i\gamma \cdot \partial - m) \psi + \frac{1}{2}(\partial\sigma)^2 - \frac{1}{2}m_\sigma\sigma^2 \\ & - \frac{1}{4}\Omega_{\mu\nu}\Omega^{\mu\nu} + \frac{1}{2}m_\omega^2\omega^2 - \frac{1}{4}\vec{R}_{\mu\nu}\vec{R}^{\mu\nu} + \frac{1}{2}m_\rho^2\vec{\rho}^2 - \frac{1}{4}F_{\mu\nu}F^{\mu\nu} \\ & - g_\sigma\bar{\psi}\sigma\psi - g_\omega\bar{\psi}\gamma \cdot \omega\psi - g_\rho\bar{\psi}\gamma \cdot \vec{\rho}\vec{\tau}\psi - e\bar{\psi}\gamma \cdot A\frac{(1 - \tau_3)}{2}\psi\end{aligned}$$

Compete well with non-relativistic models.

Determination of parameters in nuclear density functionals

Depending on sophistication of the density functional, 10-20 parameters have to be fixed by fit to experimental data.

No reliable theoretical derivation of these parameters, yet.

Recall: High-precision potentials have about 40 parameters.

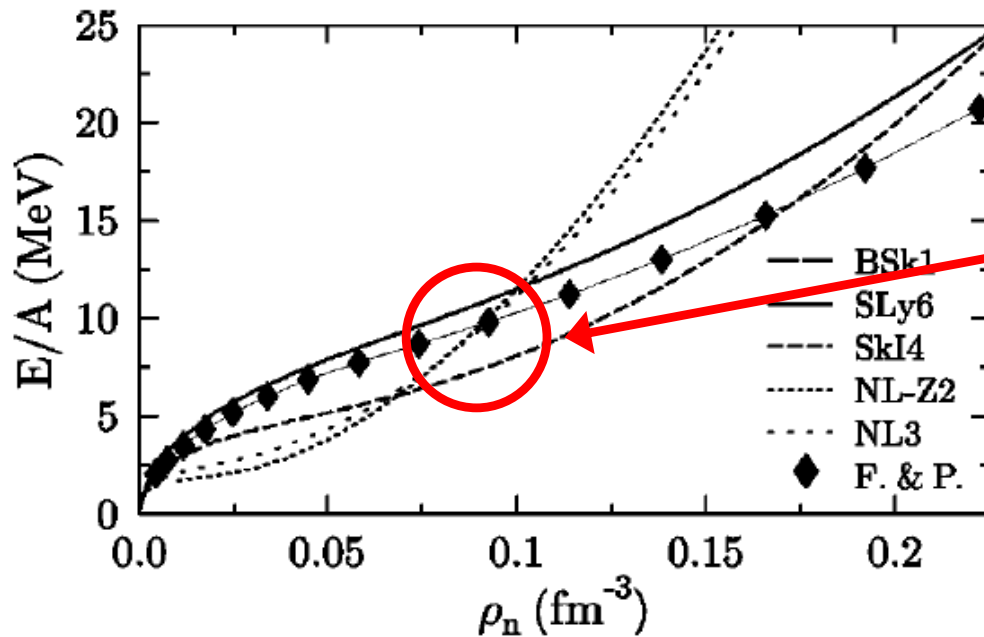
RMS error on masses:

0.7MeV fit to entire mass table

2 MeV from fit to few nuclei.

| Method | Skyrme | N_{par} | Data | σ_{rms} (MeV) |
|-----------|--------|------------------|-------------------------------------|-----------------------------|
| ETFSI | SkSC4 | 11 | 1492 ($A \geq 36$) | 0.736 |
| | | | 1374 ($Z \geq 26$) | 0.720 |
| ETFSI | SkSC4o | 11 | 1492 ($A \geq 36$) | 0.736 |
| | SkSC14 | 11 | 1492 ($A \geq 36$) | 0.795 |
| | SkSC15 | 11 | 1492 ($A \geq 36$) | 0.741 |
| ETFSI | SkSC11 | 12 | 1492 ($A \geq 36$) | 0.715 |
| ETFSI-2 | SkSC18 | 11 | 1719 ($A \geq 36$) | 0.709 |
| HFBCS1 | MSk1 | 14 | 416 (sph) | 0.848 |
| HFBCS1 | MSk2 | 14 | 416 (sph) | 0.816 |
| HFBCS1 | MSk3 | 14 | 416 (sph) | 0.784 |
| HFBCS1 | MSk4 | 14 | 416 (sph) | 0.730 |
| HFBCS1 | MSk5 | 14 | 416 (sph) | 0.709 |
| HFBCS1 | MSk6 | 14 | 1719 ($A \geq 36$) | 0.754 |
| HFBCS1 | MSk7 | 14 | 1719 ($A \geq 36$) | 0.701 |
| HFBCS1 | MSk7 | 14 | 1772 ($A \geq 36$) | 0.680 |
| HFBCS1 | MSk7 | 16 | 1888 $Z, N \geq 8$ | 0.738 |
| HFBCS | MSk7 | 16 | 1754 | 0.732 |
| HFBCS | MSk8 | 14 | 1772 ($A \geq 36$) | 0.694 |
| HFBCS | MSk9 | 14 | 1772 ($A \geq 36$) | 0.747 |
| | MSk5* | 14 | 416 (sph) | 1.141 |
| | SkSP.1 | 20 | 416 (sph) | 0.764 |
| HFB | MSk7 | 16 | 1754 ($A \geq 16$), $ N - Z > 2$ | 0.946 |
| | BSk1 | 16 | 1754 ($A \geq 16$), $ N - Z > 2$ | 0.772 |
| | BSk1 | 16 | 1888 ($A \geq 16$) | 0.764 |
| HFB-1 | BSk1 | 16 | 1768 | 0.740 |
| HFB-1 | BSk1 | 16 | 1888 ($A \geq 16$) | 0.766 |
| HFB-1(W1) | BSk1 | 16 | 1768 | 0.733 |
| HFB-1(W2) | BSk1 | 16 | 1768 | 0.702 |
| HFB-2 | BSk2 | 18 | 2135 | 0.674 |
| HFB-2' | BSk2' | 18 | 1768 | 0.651 |
| HFB-3 | BSk3 | 21 | 2135 | 0.656 |
| HFB-4 | BSk4 | 19 | 2135 | 0.680 |
| HFB-5 | BSk5 | 21 | 2135 | 0.675 |
| HFB-6 | BSk6 | 19 | 2135 | 0.686 |
| HFB-6 | BSk6 | 20 | 2135 | 0.684 |
| | | | 2149 | 0.666 |
| HFB-7 | BSk7 | 21 | 2135 | 0.676 |
| HFB-8 | BSk8 | 21 | 2135 | 0.659 |
| HFB-8 | BSk8 | 21 | 2149 | 0.635 |
| HFB-9 | BSk9 | 21 | 2149 | 0.733 |

Equation of state for pure neutron matter

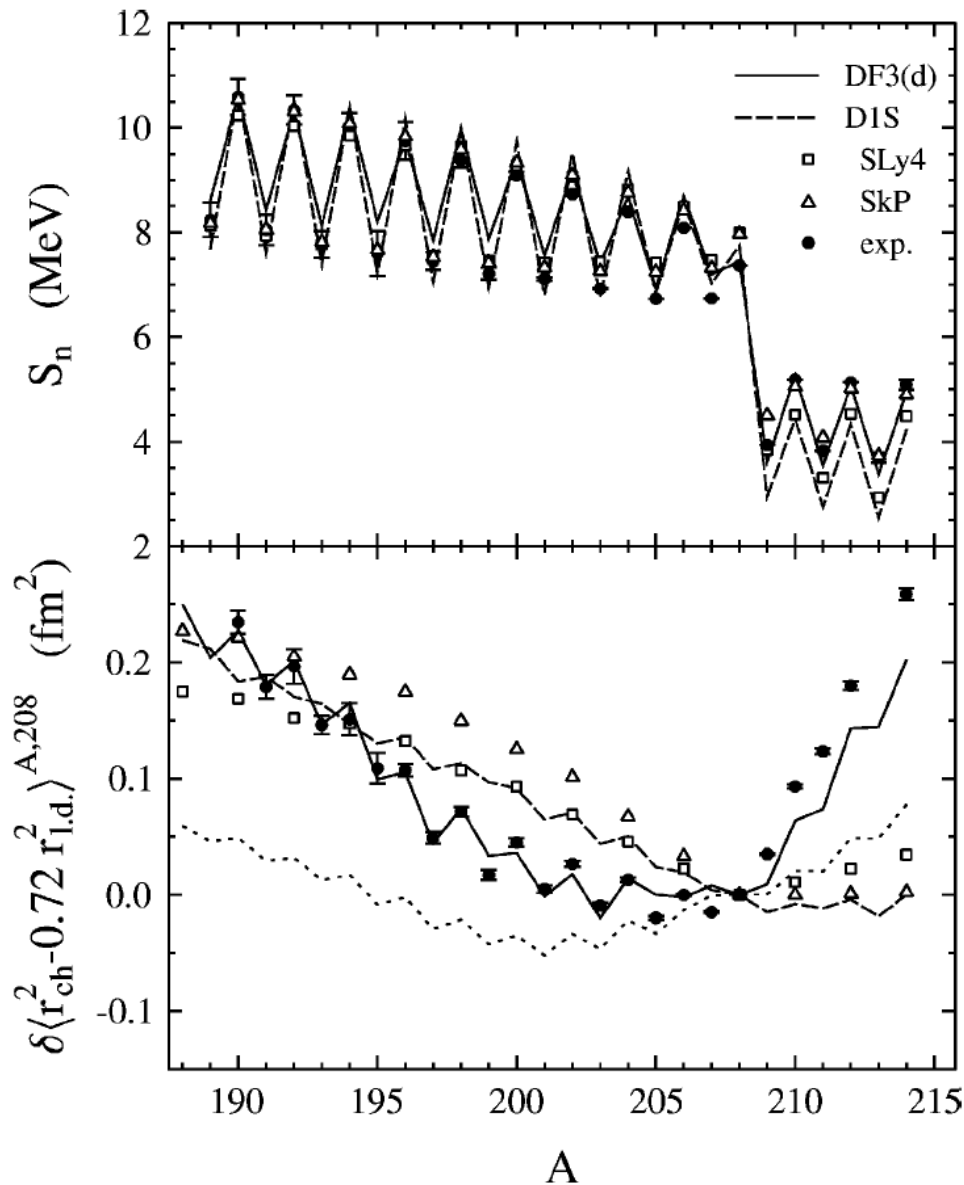


Different parametrizations yield similar results close to saturation density.

FIG. 2. Energy per particle in pure neutron matter (at zero temperature) calculated with the effective interactions as indicated: Filled diamonds connected by a thin solid line denote results from a variational many-body calculation (Friedmann and Pandharipande, 1981) which are widely used as reference data for neutron matter.

Neutron separation energies and charge radii in Pb isotopes

S.A. Fayans et al. / Nuclear Physics A 676 (2000) 49–119

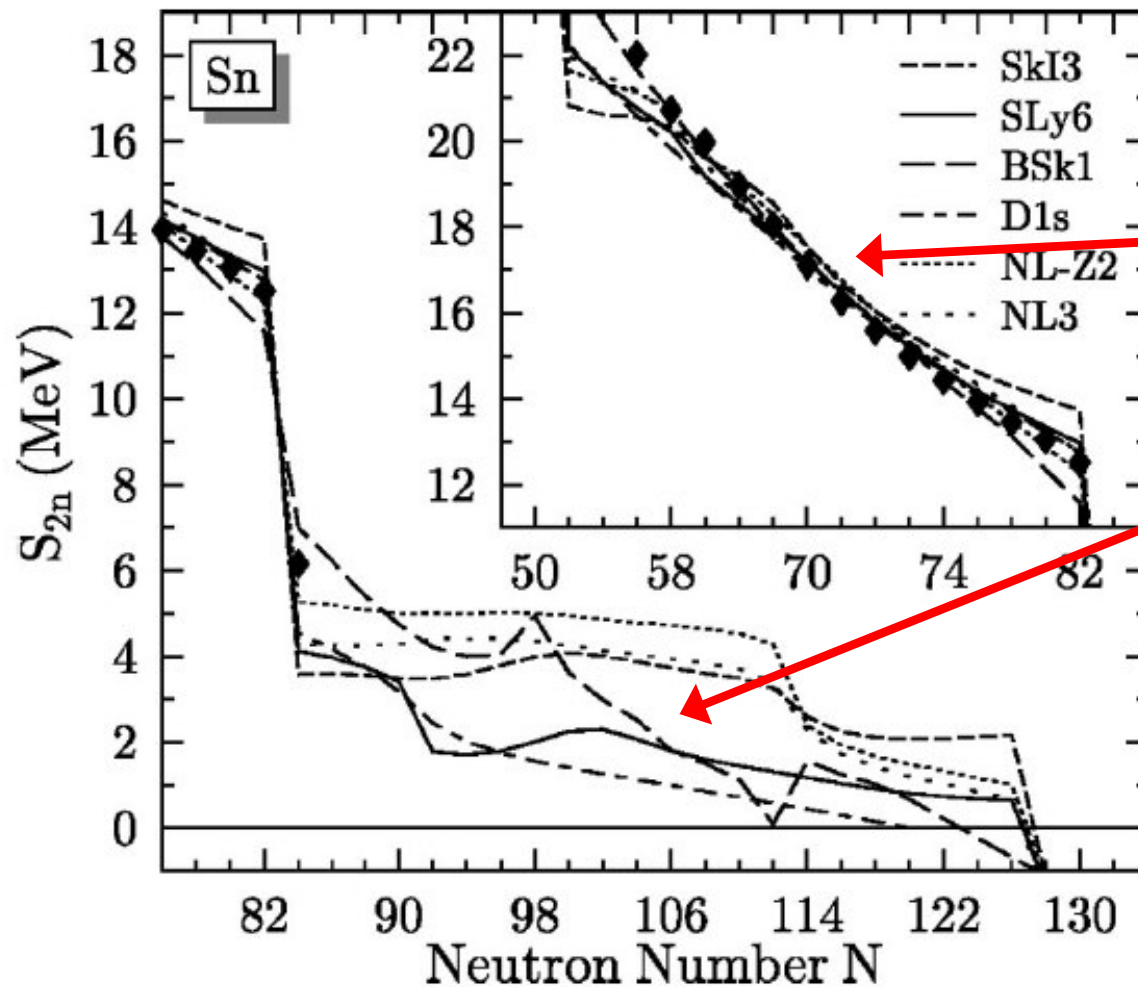


Odd-even staggering in S_n well reproduced.

Staggering of charge radii accurately reproduced.

Fayans' density functional describes pairing effects very well.

Two-neutron separation energy in Sn isotopes



Good agreement with experiment where data exists (partly input to functional)

Divergent results in extrapolations.

Nuclei close to drip line magnify aspects that are poorly modeled so far!

FIG. 5. Two-neutron separation energy S_{2n} for the chain of tin isotopes. The inset on the upper right shows results for $N \leq 82$.

Radii of charge distributions

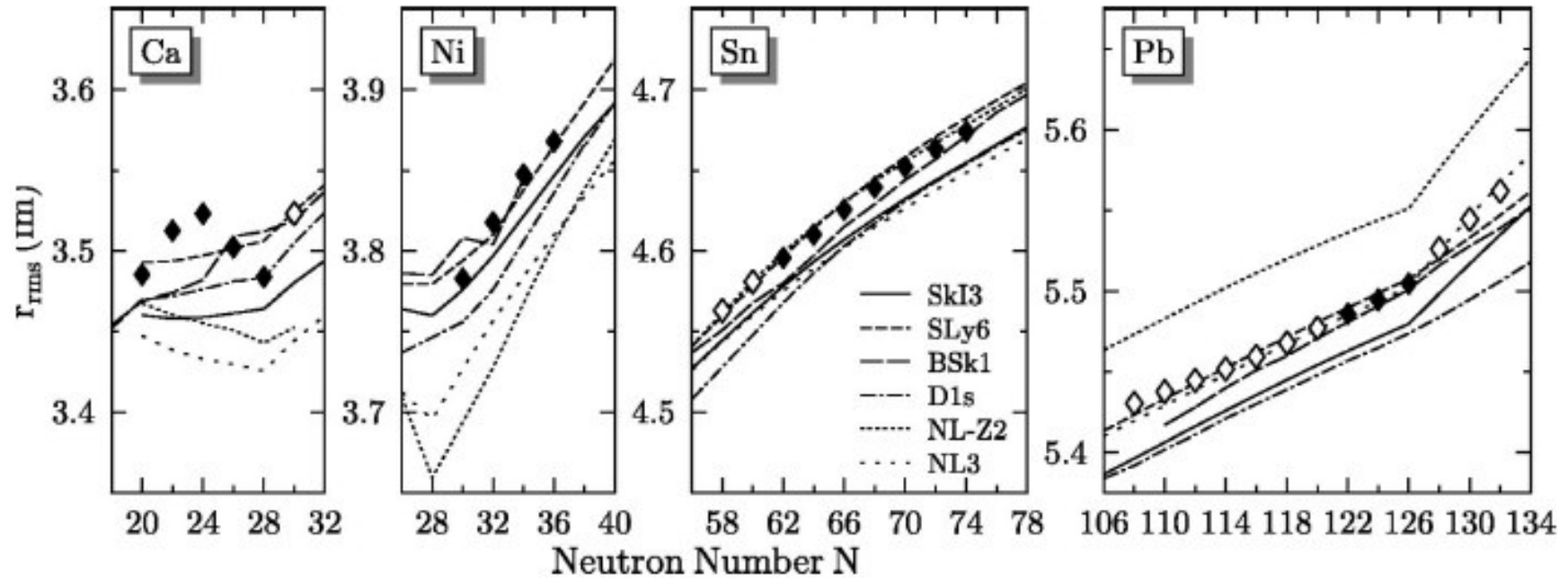
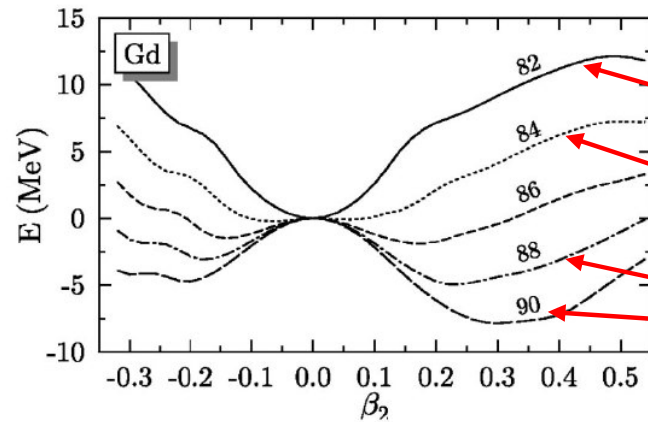


FIG. 11. Comparison of rms radii of the charge distributions from spherical mean-field calculations. Experimental data are taken from Nadjakov *et al.* (1994). Filled diamonds denote results from direct radius measurements, while open diamonds are obtained from measurements of isotopic shifts.

Shape transitions in Gd isotopes

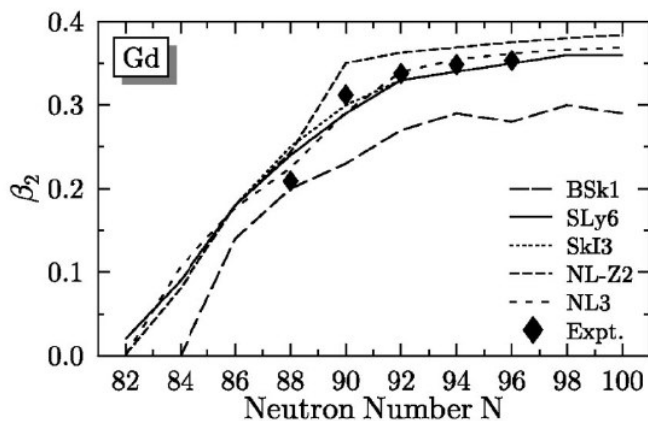


Potential energy surfaces

spherical

transitional

deformed

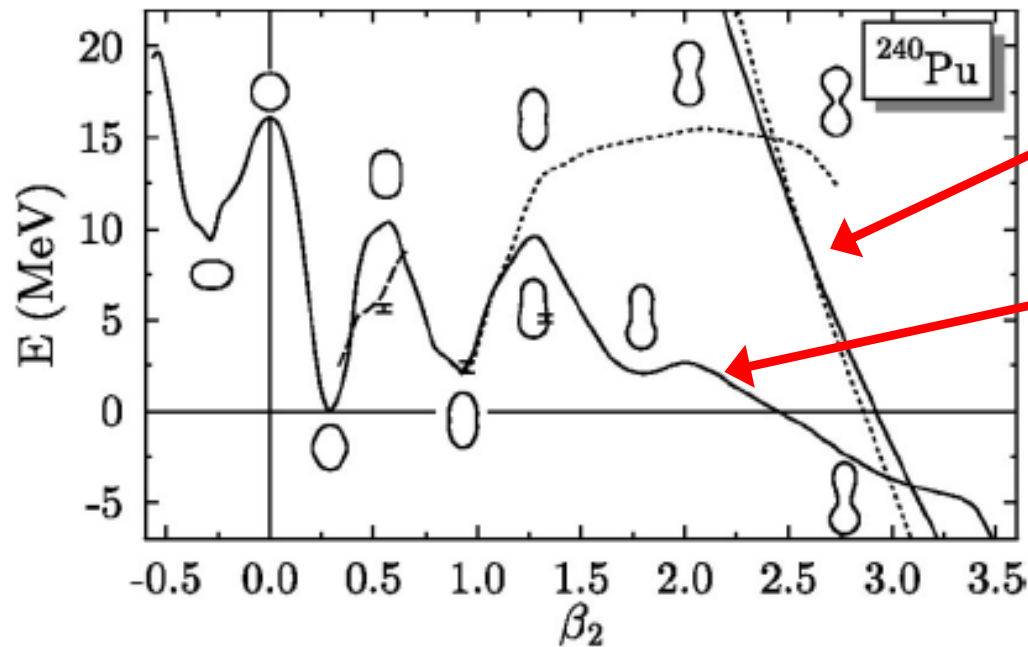


Shape transitions commonly encountered in Rare Earth nuclei.

→ Interacting boson model and dynamical symmetries.

FIG. 13. Transition from spherical to deformed shapes in the chain of Gd isotopes. Upper panel: HF+BCS potential-energy surfaces calculated with the SLy6 interaction for neutron numbers ranging from 82 to 90. Lower panel: Ground-state deformation of Gd isotopes for several forces. Pairing is treated with the BCS method except for BSk1 for which the HFB method is used. Experimental values are taken from Raman *et al.* (2001).

Fission barriers



Fusion paths

Fission paths:

Relaxing symmetries (on possible shapes/deformations) typically lower the energy.

Mean-field model exaggerate barriers when compared to date.

Recall: exponential sensitivity of tunneling rate on barrier height.

FIG. 15. Paths in the deformation energy landscape of ^{240}Pu calculated with the SkI4 interaction. The solid line corresponds to axial quadrupole and octupole (reflection asymmetric) constraints, the dashed line to triaxial quadrupole constraints, the dotted line to axial quadrupole constraint only. The two steep lines correspond to the symmetric (dotted line) and asymmetric (solid line) fusion paths. Shapes along the paths are indicated by the density contours at $\rho_0 = 0.07 \text{ fm}^{-3}$. From Bender (1998).

Shape coexistence in superheavy nuclei

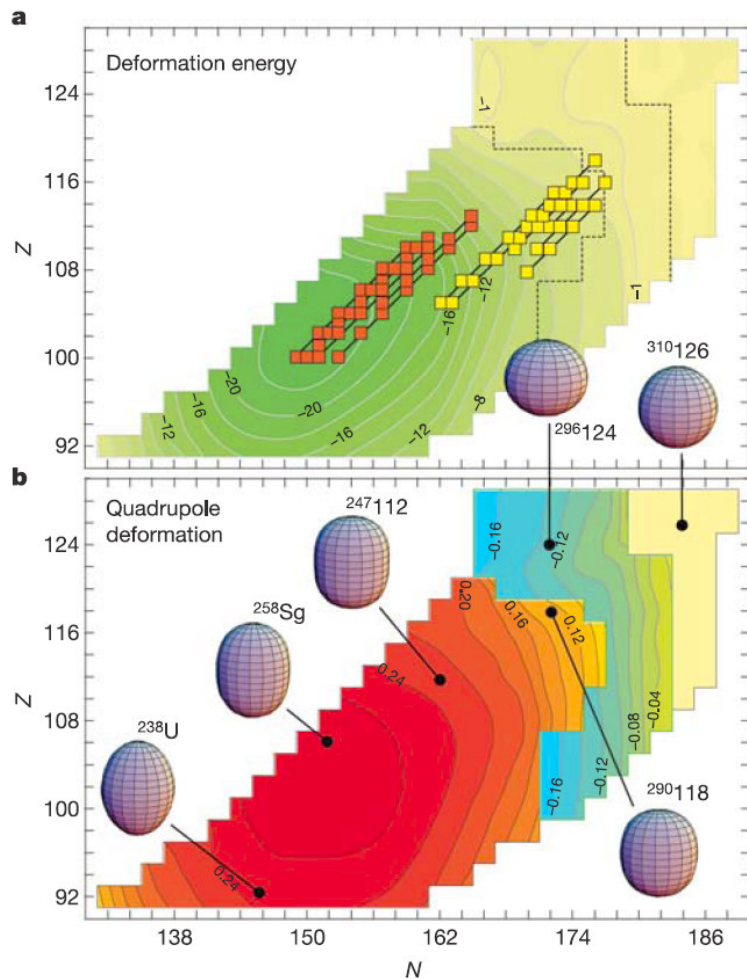


Figure 1 Deformation properties of even–even superheavy nuclei calculated self-consistently in the (N, Z) -plane with the SLy4 nuclear energy density functional. The centre of the shell stability is predicted around $N = 184$, $Z = 126$. **a**, Deformation energy (in MeV) defined as a difference between the ground-state energy and the energy at the spherical shape. The $Z = 110$ – 113 α -decay chains found at GSI and RIKEN are marked by red squares. The $Z = 118$, 116 , 115 and 114 unconfirmed α -decay chains reported in Dubna are marked by yellow squares. **b**, Predicted ground-state mass quadrupole deformation β_2 (extracted using equation (7) of ref. 6 from the calculated axial mass quadrupole moment Q_{20}) and corresponding nuclear shapes for selected nuclei. Prolate shapes ($\beta_2 > 0$) are coloured red–orange, oblate shapes ($\beta_2 < 0$) are blue–green, and spherical shapes ($\beta_2 = 0$) are light yellow.

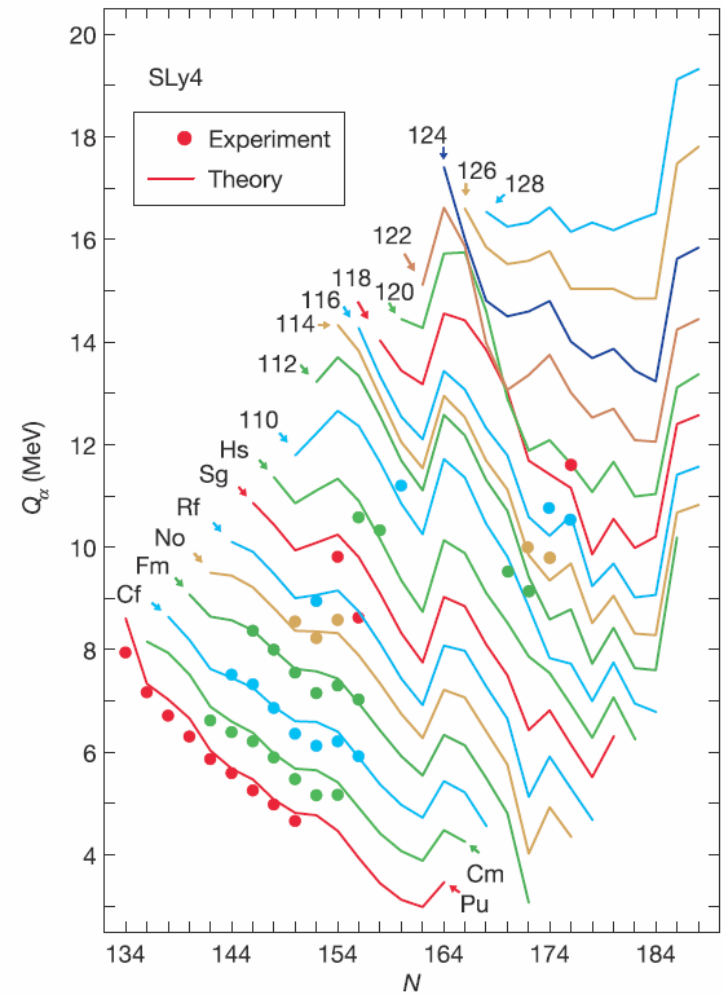


Figure 2 Q_α values for even–even nuclei with $96 \leq Z \leq 118$ obtained in the self-consistent calculations using the energy density functional SLy4. They are compared to experimental data (closed symbols), including the recent Dubna–Livermore data on the $Z = 116$ and 118 α -decay chains^{23,24}. The irregular behaviour of Q_α as a function of particle numbers can be attributed to shell effects and the resulting deformation changes. (After ref.1.)

Summary

Self-consistent mean-field models

- Theoretical foundation within Kohn-Sham DFT.
- Applicable across nuclear chart.
- Phenomenological approach; fit to data.
- Yield impressive results (given their simplicity) in regions that entered the fit.
- Form of functional needs improvement to cover drip line physics
- Future theoretical and experimental advances for neutron-rich nuclei necessary.